Technical Implementation of SMOS Data in the ECMWF Integrated Forecasting System

Joaquín Muñoz Sabater, *Member, IEEE*, Anne Fouilloux, and Patricia de Rosnay

***Abstract*—The launch of the Soil Moisture and Ocean Salinity (SMOS) satellite of the European Space Agency opens the way to using a new type of satellite data that are very sensitive to soil moisture for numerical weather prediction. The European Centre for Medium-Range Weather Forecasts (ECMWF) has developed an operational chain which makes it possible to process SMOS data in near real time (NRT) and compare it with a model equivalent. This process has been very challenging. The main reasons are the particular characteristics of the SMOS observation system and the large volume of data. Despite these obstacles, SMOS data are being processed successfully in NRT within the ECMWF Integrated Forecasting System (IFS). The ultimate objective is to assimilate these data in the IFS. It is expected to have an impact on the weather forecast at short and medium ranges. Prior to assimilation experiments, the quality of the data has to be assessed. This can be done through monitoring activities. Monitoring is a routine task performed with all satellite data, and among other things, it makes it possible to localize temporal (or spatial) bias or drifts in the data, thus providing NRT reports to the calibration and validation teams, which can act accordingly. In this letter, the implementation of SMOS data in the ECMWF IFS for monitoring purposes is discussed. The system was developed using a simulated file for the NRT processor, and it was tested using real data from the first year since the launch date.**

***Index Terms*—European Centre for Medium-Range Weather Forecasts (ECMWF), implementation, monitoring, Soil Moisture and Ocean Salinity (SMOS).**

I. Introduction

THE SUCCESSFUL launch of the Soil Moisture and Ocean Salinity (SMOS) satellite of the European Space Agency [1] is already providing an unprecedented new source of remotely sensed data that are sensitive to soil moisture over land and salinity over the oceans. Soil moisture has been extensively identified as a critical land variable due to its strong influence in the exchanges of water, energy, and carbon fluxes at the interface between the soil, vegetation, and the lowest level of the atmosphere [2]. A good estimation of soil moisture has a direct impact on precipitation and air temperature predictability at short and medium ranges [3], [4].

Passive L-band measurements are the most suitable ones for soil moisture retrievals. In this microwave region, attenuation from clouds and vegetation is smaller than that at higher frequencies [5]. Nonetheless, the heavy cost and technological challenge of arranging a large antenna in L-band have prevented an earlier spatial L-band mission. For SMOS, an antenna of approximately 8 m in diameter would be necessary to meet the spatial resolution requirements of the mission [1], making the cost prohibitive with the current technology. In SMOS, this problem is overcome by applying the interferometric technique. Instead of one large antenna, 69 little receivers installed in three deployable Y-shaped arms of 3.5-m length collect the radiation emitted by the Earth's surface between 1400 and 1427 MHz. The phase difference measured between the individual receivers makes it possible to reconstruct an image which meets the science requirements, i.e., volumetric soil moisture with an accuracy of 0.04 m^3/m^3 and a spatial resolution of 40–50 km [6]. As a numerical weather prediction (NWP) center, the European Centre for Medium-Range Weather Forecasts (ECMWF) is receiving a near-real-time (NRT) product, which is automatically recovered from the SMOS Data Processing Ground Segment. To fully take advantage of this product, ECMWF has implemented this new data type in the Integrated Forecasting System (IFS), which opens the possibility to monitor and assimilate the data within the IFS. This is a challenging task. In SMOS, the interferometric technique applied makes it possible to observe the same area under different views, thus providing multiangular and multipolarized observations of the same scene at different time stamps. Up to 150 records of brightness temperatures (T_B) between 0° and 65° are provided per observed area. The angular resolution of the observations is very high. This measuring principle has the following two consequences: 1) the distribution of a unique data set with new features very different to any other source of satellite data used for NWP and 2) the production of a very large volume of data which cannot all be ingested in the IFS. Therefore, the data volume must be reduced significantly before a model equivalent is computed and compared with the observations. The previous characteristics of the SMOS observation system have raised great concern about the feasibility of integrating SMOS data in a complex NWP system. In this letter, the feasibility of its operational use is demonstrated. The main steps involved in the design of the SMOS data process chain are presented. The objective is to set up the structure necessary to operationally produce a comparison between a subgroup of SMOS observations and their model equivalent, as this is the main input for an assimilation scheme. The chain developed was tested with the first flow of available data and run successfully for one year.

II. Data Product Used at ECMWF

The product used at ECMWF is the NRT which constitutes geographically sorted swath-based maps of T_B. The geolocated product received at ECMWF is arranged in an equal area grid

Manuscript received March 11, 2011; revised June 21, 2011; accepted August 2, 2011. This work was supported by the European Space Research Institute of the European Space Agency under Contract 20244/07/I-LG.

The authors are with the European Centre for Medium-Range Weather Forecasts, RG2 9AX Reading, U.K. (e-mail: joaquin.munoz@ecmwf.int; Anne.Fouilloux@ecmwf.int; Patricia.Rosnay@ecmwf.int).

Digital Object Identifier 10.1109/LGRS.2011.2164777

system called ISEA 4H9 (Icosahedron Snyder Equal Area grid with aperture 4 at resolution 9) [7]. For this grid, the centers of the cell grids are at equal distances of 15 km over land, with a standard deviation of 0.9 km. Over oceans, the grid has a coarser resolution, which is half of the resolution over land, as oceans are more homogeneous than continental surfaces. The data are organized in messages. Each message corresponds to a snapshot where the integration time is 1.2 s, as this is the time in which all correlations of a single scene are measured. On average, each message contains around 4800 observations over land if the instrument runs in dual-polarization mode. In this running mode, data set records are generated alternately each 1.2 s at horizontal (HH) and vertical (VV) polarizations. In full-polarization mode, all four Stokes parameters of the radiation are collected by the antennas during four consecutive integrations. Thus, the polarization state of the radiation is fully described in this mode. Since the end of the commissioning phase, the instrument on-board SMOS has been operating only in full-polarization mode.

III. Implementation

In this section, the main steps and challenges involved in the implementation of SMOS data in the IFS are addressed. Before SMOS data can be assimilated, the data go through a series of tasks which have the objective of validating and comparing the observations with a simulated value, thus producing an input for the soil moisture assimilation scheme. These tasks can be classified into the following two large groups:

1) data prescreening;
2) computations in the model grid.

A. Data Prescreening

First, NRT raw data (see Section II) processed at the European Space Astronomy Centre in Madrid (Spain) are retrieved and slightly modified to feed the prescreening tasks. These tasks perform quality control checks.

1) Generic checks: Files which do not contain crucial header information are rejected. It is checked that date and time are complete, geographic coordinates are not missing, and instrument data correspond to SMOS data.
2) The validity of data is checked: Individual observations are checked to be in a correct geographical position, and T_B is checked to be in the range of physically reasonable values (not lower than 50 K and not greater than 350 K), which is also a practical hard radio-frequency interference (RFI) filter.
3) Data are thinned to reduce the volume of SMOS data processed within the IFS.

Data thinning is a critical step insofar as it selects not only which data from the original files will be monitored but also which data could be used to correct the soil moisture state through an assimilation experiment. The daily volume of SMOS data arriving in ECMWF archives in NRT is of about 8 GB, which is by far one of the greatest sources of satellite data received at ECMWF. This amount of data cannot be introduced in the IFS for just one single satellite instrument, taking into account that data from many other satellites are used simultaneously. For SMOS, only 5%–10% of the initial data volume

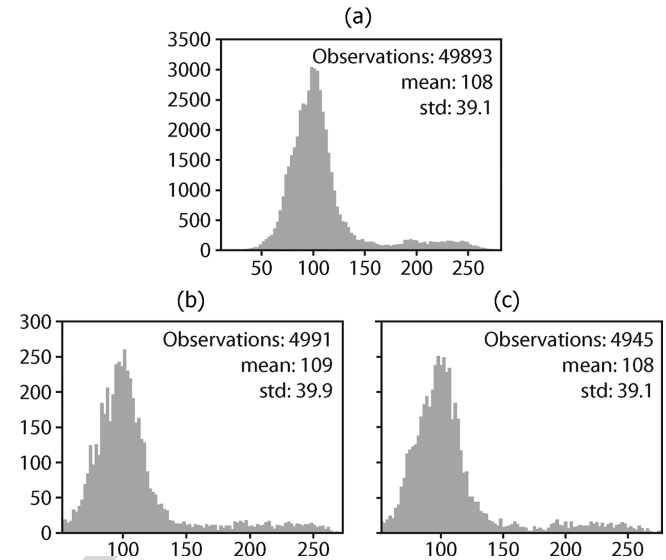

Fig. 1. Histograms of brightness temperatures for an SMOS-simulated file for December 17, 2010. (a) Histogram of T_B for testing file. (b) Histogram of T_B for EXP1. (c) Histogram of T_B for EXP2.

can realistically be ingested in the IFS. Thinning is therefore a mandatory step and also prevents redundant observations in the assimilation system.

Data can be thinned in many different ways. For monitoring purposes, the thinned subset of observations should be representative and keep the same statistical characteristics as the original data set. In this letter, two simple experiments are shown in order to investigate the characteristics of a thinned subset of SMOS observations. In the first experiment (EXP1), only observations containing integer incidence angles $\pm 0.1^\circ$ are selected. This offset parameter was tuned in order to filter approximately only 10% of the initial number of observations. The rationale for this filter is that, even though the surface emission is not a linear process with the incidence angle, the land microwave emission should not be very sensitive to small differences in the angular illumination of the target. Thus, a significant data reduction should be achieved while keeping the original angular signature of the observations. In the second experiment (EXP2), a simple filter which keeps only one out of ten observations from a snapshot was applied. This is a practical way to keep, roughly, only 10% of the original data volume, making it compatible with the IFS memory capabilities.

With a view to implementing a thinning filter in the IFS, these two experiments were tested with an SMOS-simulated NRT file for December 17, 2010. That was the only data available. This file contains several snapshots covering mostly the Arabian Sea but also some land in Oman and Saudi Arabia. In total, it has a volume of 1 067 724 B, corresponding to 48 993 observations. The histogram of simulated T_B is shown in Fig. 1(a). It clearly shows the sea (predominantly) and land features. The mean is 108 K, whereas the standard deviation is 39.1 K. Fig. 1(b) and (c) shows the histograms of T_B for EXP1 and EXP2, respectively. In EXP1, exactly 10% of the initial data set was selected, whereas in EXP2, 9.91% was selected. For EXP2, the statistics remain as in the original data set, whereas in EXP1, they are slightly degraded. The main advantage of EXP2 is that all incidence angles are still available for monitoring purposes and it allows greater flexibility for further processing. For example,

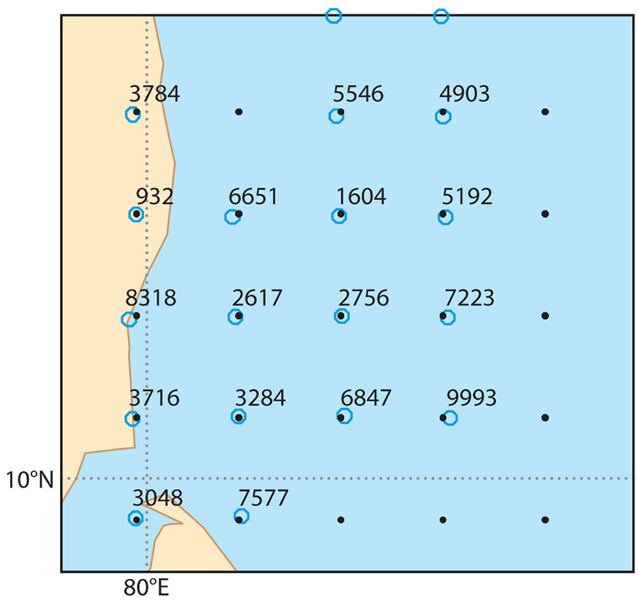

Fig. 2. (Blue circles) Nearest SMOS observations to the (black dots) ECMWF T159 model grid points. The values are the distances between grid points and the nearest SMOS observation, in meters.

by using EXP2, data can be averaged in angular bins at later steps. Furthermore, the implementation is very simple, and only one parameter is needed to control this filter. For EXP1, the offset parameter has to be optimized each time to control the number of observations filtered, and not all angular geometries can be monitored. Thus, the initial implementation of a filter type as in EXP2 was preferred for monitoring purposes. Due to operational constraints, this process has to be completed very quickly. On average, 12 h of data are processed in almost 1 min using eight processors in parallel. This makes SMOS prescreening tasks fully compatible with the current ECMWF operational system.

B. Computations in the Model Grid

The implementation of SMOS data monitoring in the IFS was carried out in the model grid. This has several advantages.

1) All the background fields necessary to simulate T_B at the top of the atmosphere are computed and available in the model grid point space. Thus, it avoids interpolating physical quantities to an observation location.
2) Other satellite data that are sensitive to soil moisture, such as AMSR-E data in C-band, are also available in the model space, making a comparison with other satellite data possible. The subset of observations which are selected after the prescreening filters undergoes (roughly) a two-step process.

a) Observations are brought into the model grid point space at the required model resolution by using the nearest neighbor technique. At the same time, a mask of the flags containing information of the grid point is created. Fig. 2 shows the SMOS observations for the simulated file on December 17, 2010, collocated to the nearest grid point. For the sake of clarity, a magnified area over the south Indian coast is shown, and a rather coarse grid T159 is used (~125 km). The distance limit beyond which observations are rejected was set to 10 000 m. The number of observations monitored depends on the model grid resolution and the distance limit parameter. At T799 (~25 km) or higher spectral resolution, SMOS observations within the distance limit were found for all grid points (not shown).
b) For each observation flagged as being the closest to a model grid point, a background value is simulated with an L-band forward model operator. Thus, the innovation vector is obtained as the main input for a soil moisture analysis. The forward model interfaced to the IFS is the Community Microwave Emission Model [8], [9], as explained in [10].

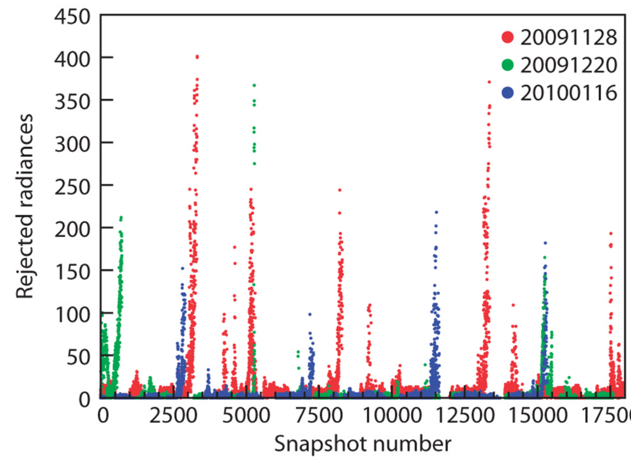

Fig. 3. Number of rejected observations in the prescreening tasks for 6 h of NRT SMOS data.

IV. RESULTS WITH REAL DATA

The operational chain described in Section III was tested with real T_B data from the commissioning phase. No distinction between ascendant and descendent orbits was made. These data sets were the following:

Data set 1) November 28, 2009;
Data set 2) December 15, 2009;
Data set 3) December 20, 2009;
Data set 4) January 16, 2010.

A. Prescreening Results and Model Equivalent

The quality checks listed in Section III-A were tested with data sets 1), 3), and 4). Fig. 3 shows the number of individual T_B values rejected as a function of the first 18 000 snapshots. This corresponds to the first 6 h of collected data for these days. During the commissioning phase, the SMOS operational mode was alternated between dual and full polarizations so as to test and select the optimal mode for the instrument. Data sets tested in this section contain data in both modes. Thus, for comparison purposes, only snapshots with fewer than 5000 subsets were used because they correspond to pure HH- or VV-polarization integrations. This figure clearly shows that the number of rejected radiances is the greatest for November 28, when the data were not yet calibrated, whereas the number is significantly reduced for December 20 and January 16. Table I shows a quantitative comparison between the three data sets. It

TABLE I
NUMBER OF OBSERVATIONS REJECTED FOR 6 h OF DATA DURING THE EARLY QUALITY CHECK PHASE

Date	snapshots	subsets	rejections	% rejected
28-11-2009	17940	28203176	147185	0.52
20-12-2009	17592	28739029	58967	0.21
16-01-2010	15347	24322415	34386	0.14

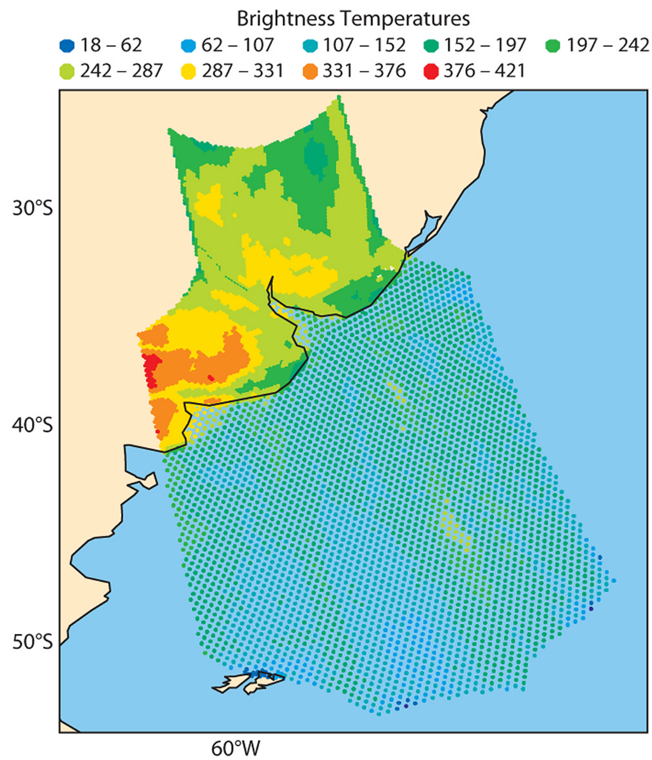

Fig. 4. Brightness temperatures over the east of Argentina (in kelvins), in VV polarization for an NRT file received December 15, 2009.

TABLE II
THINNING FILTERS EXP1 AND EXP2. "NBR OBS" IS THE NUMBER OF OBSERVATIONS, "MEAN" IS THE BRIGHTNESS TEMPERATURE MEAN VALUE (IN KELVINS), AND "STD" IS THE STANDARD DEVIATION

	Original file	after EXP1	after EXP2
Nbr obs	522566	52589	52306
mean	189	191	189
STD	63.7	63.1	63.5

shows how the quality of the data is the best in January 2010, with only 0.14% of observations rejected after the first group of quality checks. Although this percentage is small in November, it is relatively more significant than those in December 2009 and January 2010.

Data set 2) was used to test the thinning filters described as EXP1 and EXP2 in Section III-A. In total, this file contains only 211 snapshots (southeast Argentinian coast) with 537 132 observations (Fig. 4). The results are summarized in Table II for the VV polarization. The results for HH polarization were equivalent. In both cases, the number of observations filtered was very similar. For EXP2, the statistical signature of the thinned subset is closer to that of the original data set, but more importantly, there is still the possibility to monitor any incidence angle. With this single filter, on average, ten angular observations are considered for each grid point. In contrast to an EXP1-type filter, this filter approach has better control over the volume of the filtered data set. By using a series of processors in parallel, the collocation to the model grid is performed quickly and efficiently. At this stage, each model grid point is associated with the closest observation, as long as it is within the distance limit parameter. Then, for each grid point, the geometry of the closest observation is used to compute a model equivalent and compare it with the observation. At the end of this process, each grid point is associated with at least one model equivalent.

B. *Continuous Monitoring of SMOS Observations*

The feasibility of using the previous chain operationally was tested with several months of real data. SMOS data were monitored by systematically producing global maps of NRT T_B for different incidence angles (0, 10, 20, 30, 40, 50, and 60) and for both HH- and VV-polarization modes. Plots for 2010 are available at http://www.ecmwf.int/research/ESA_projects/SMOS/monitoring/2010/2010.html. A simple inspection of these figures makes it possible to observe not only the angular evolution of the data for each polarization state but also a significant improvement in the quality of the observations, specially after the instrument was calibrated. Fig. 5 shows T_B at 40° incidence angle and VV-polarization state for days 1 (top), 3 (middle), and 4 (bottom). It shows a clear evolution in the quality of the data, from day 1 (top) to day 4 (bottom). The day in November (top) is shown to be very noisy. These were data received within the first two weeks of the instrument "Switch-On Phase," which obviously had not benefited yet from a good calibration. In December, a major calibration event took place, and the difference in the product is quite significant when comparing the top and middle figures. Improvements are present almost everywhere. The data are even better for January 16, although this needs a closer examination and quantitative results to confirm it (see Table I). Results for the HH polarization were equivalent. As SMOS is a research mission, it was also important to check the correct functioning of the novel instrument. Hence, it was checked that the T_B values got colder with increasing the incidence angle for HH polarization, and the opposite behavior was shown for the VV polarization (see, for example, the online plots), with both displaying values within an acceptable physical range. It is also an objective of data monitoring activities to report on possible spatial or temporal effects on the data: The most outer sides of the satellite track look colder than the inner part, which is due to the extended alias-free field of view, of lower quality than data closer to the center of the track. There is still residual RFI over Europe, the Middle East, and Asia, which is particularly straightforward to spot when the data look very "red" and noisy. The data are of relatively better quality over the whole of America, Australia, and southern Africa.

V. SUMMARY

Integrating a new type of satellite data with innovative features in a complex NWP system and making it fully compatible with an NRT structure is a very challenging task. This is the case for the SMOS NRT product arriving at ECMWF. The large volume of SMOS data and the large number of angular views per pixel have raised concerns about the feasibility of using this product in an operational NWP context. Despite these challenging features, the operational use and the feasibility of

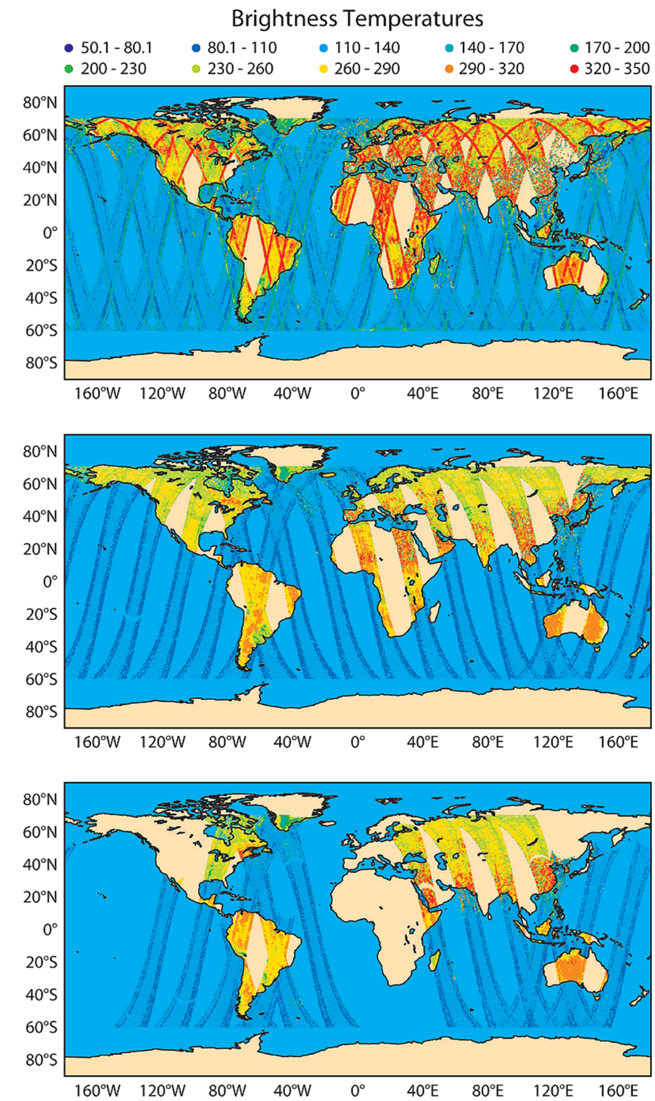

4/C

Fig. 5. Brightness temperatures for NRT SMOS data at 40° incidence angle and VV-polarization state. The figure on the top is for November 28, 2009, the middle figure corresponds to December 20, 2009, and the bottom figure corresponds to January 16, 2010.

processing a large amount of SMOS data in NRT were shown. The objective was to set up the structure required to compare SMOS measurements with a model equivalent. This opens the possibility of investigating the benefits that these observations can bring for weather forecast skill. Thus, rather than providing an exhaustive analysis of the observations, this letter is more oriented toward demonstrating that the SMOS data monitoring chain is efficient and compatible with an NRT system.

The operational chain proposed in this letter is able to cope with more than 8 GB of SMOS data a day, i.e., more than 300 million observations. Each observation is subjected to an exhaustive quality control; then, the whole data set is strongly thinned. Although the thinning filter proposed is quite simple (keeping only one out of ten observations), it keeps all the incidence angles (for monitoring purposes) and has good control over the size of the filtered data set. However, the optimal thinning filter to be applied to the data is not obvious. For example, possible approaches may include averaging the data within predefined angular bins, discarding snapshots where a grid point has a T_B value exceeding a given threshold, or removing noisy data at low incidence angles. Certainly, the development of an enhanced thinning filter deserves further investigation, and it is a key activity as assimilation experiments may depend strongly on the selected subsample of data.

Forward modeling on the model grid (using the geometry of the nearest SMOS observation) proved to be efficient and fast if several processors were used simultaneously. The analysis of the first batch of real data using this structure proved to be useful. It suggested a clear enhancement in the data quality during the first months of the mission, both qualitatively and quantitatively. There are still strong sources of RFI remaining in Europe and Asia, whereas a visible data degradation is still observed at the edges of the satellite track over oceans at high incidence angles. The systematic production of these plots in NRT is an excellent way to monitor the data just a few hours after sensing time and to quickly inform calibration and validation teams about trends or drifts in the data. In this context, SMOS data monitoring will be supported through the provision of the statistics of the modeled values in the grid point space, where first-guess departures are computed. These statistics are currently being obtained for several weeks of data, and their analysis will be presented in a follow-up paper totally devoted to this aspect.

Acknowledgment

The authors would like to thank M. Dragosavac, I. Mallas, and A. Hofstadler for their support with the production of the preprocessed data within the near-real-time chain and the anonymous reviewers for the useful comments.

References

[1] Y. Kerr, P. Waldteufel, J.-P. Wigneron, S. Delwart, F. Cabot, J. Boutin, M. Escorihuela, J. Font, N. Reul, C. Gruhier, S. Juglea, M. Drinkwater, A. Hahne, M. Martin-Neira, and S. Mecklenburg, "The SMOS mission: New tool for monitoring key elements of the global water cycle," *Proc. IEEE*, vol. 98, no. 5, pp. 666–687, May 2010.

[2] J. Shukla and Y. Mintz, "Influence of land-surface evapotranspiration on the Earth's climate," *Science*, vol. 215, no. 4539, pp. 1498–1501, Mar. 1982.

[3] L. Ferranti and P. Viterbo, "The European summer of 2003: Sensitivity to soil water initial conditions," *J. Clim.*, vol. 19, no. 15, pp. 3659–3680, Aug. 2006.

[4] M. Drusch and P. Viterbo, "Assimilation of screen-level variables in ECMWF's Integrated Forecast System: A study on the impact of the forecast quality and analyzed soil moisture," *Mon. Wea. Rev.*, vol. 135, no. 2, pp. 300–314, Feb. 2007. doi:10.1175/MWR3309.1.

[5] F. T. Ulaby, R. K. Moore, and A. K. Fung, *Microwave Remote Sensing: Active and Passive. Vol. I*. Reading, MA: Addison-Wesley, 1981, p. 56.

[6] P. Waldteufel, J. Boutin, and Y. Kerr, "Selecting an optimal configuration for the Soil Moisture and Ocean Salinity mission," *Radio Sci.*, vol. 38, no. 3, p. 8051, 2009. doi:10.1029/2002RS002744.

[7] K. Sahr, D. White, and A. J. Kimerling, "Geodesic discrete global grid systems cartography," *Cartography Geographic Inf. Sci.*, vol. 30, no. 2, pp. 121–134, 2003.

[8] M. Drusch, T. Holmes, P. de Rosnay, and G. Balsamo, "Comparing ERA-40 based L-band brightness temperatures with Skylab observations: A calibration/validation study using the Community Microwave Emission Model," *J. Hydrometeor.*, vol. 10, no. 1, pp. 213–226, Feb. 2009. doi:10.1175/2008JHM964.1.

[9] P. de Rosnay, M. Drusch, A. Boone, G. Balsamo, B. Decharme, P. Harris, Y. Kerr, T. Pellarin, J. Polcher, and J.-P. Wigneron, "AMMA Land Surface Model Intercomparison Experiment coupled to the Community Microwave Emission Model: ALMIP-MEM," *J. Geophys. Res.*, vol. 114, no. D5, p. d05 108, 2009. doi:10.1029/2008JD010724.

[10] J. M. Sabater, P. Rosnay, A. Fouilloux, M. Dragosavac, and A. Hofstadler, "Milestone 1 technical note 1 part II: IFS interface," Eur. Centre Medium-Range Wea. Forecasts, Reading, U.K., Nov. 2009, Tech. Rep.

AUTHOR QUERIES

AUTHOR PLEASE ANSWER ALL QUERIES

AQ1 = This sentence was reworded for clarity. Please check if the intended meaning was retained.
AQ2 = "ESA" and "ESRIN" were defined as "European Space Agency" and "European Space Research Institute," respectively. Please check if appropriate.
AQ3 = The financial support statement was reworded to conform to IEEE style. Please check if appropriate.
AQ4 = Occurrences of the unit "Gb" were changed to "GB" (for gigabyte). Please check if appropriate.
AQ5 = List items "1/" and "2/" were captured as a displayed list for clarity in presentation. Please check if appropriate.
AQ6 = Please provide the expanded form of the acronym "AMSR-E."
AQ7 = This sentence was reworded for clarity. Please check if the intended meaning was retained.

END OF ALL QUERIES